




Communication

Hydrogen Evolution Volcano(es)—From Acidic to Neutral and Alkaline Solutions

Goitom K. Gebremariam ^{1,2,†} , Aleksandar Z. Jovanović ^{1,†}, Ana S. Dobrota ¹ , Natalia V. Skorodumova ³ and Igor A. Pašti ^{1,*} 

¹ University of Belgrade—Faculty of Physical Chemistry, Studentski trg 12–16, 11158 Belgrade, Serbia

² Department of Chemistry, Mai Nefhi College of Science, National Higher Education and Research Institute, Asmara 12676, Eritrea

³ Department of Materials Science and Engineering, School of Industrial Engineering and Management, KTH—Royal Institute of Technology, Brinellvägen 23, 100 44 Stockholm, Sweden

* Correspondence: igor@ffh.bg.ac.rs; Tel.: +381-11-3336-625

† These authors contributed equally to this work.

Abstract: As the global energy crisis continues, efficient hydrogen production is one of the hottest topics these days. In this sense, establishing catalytic trends for hydrogen production is essential for choosing proper H₂ generation technology and catalytic material. Volcano plots for hydrogen evolution in acidic media are well-known, while a volcano plot in alkaline media was constructed ten years ago using theoretically calculated hydrogen binding energies. Here, for the first time, we show that the volcano-type relationships are largely maintained in a wide range of pH values, from acidic to neutral and alkaline solutions. We do this using theoretically calculated hydrogen binding energies on clean metallic surfaces and experimentally measured hydrogen evolution overpotentials. When metallic surfaces are exposed to high anodic potentials, hydrogen evolution can be boosted or significantly impeded, depending on the type of metal and the electrolyte in which the reaction occurs. Such effects are discussed here and can be used to properly tailor catalytic materials for hydrogen production via different water electrolysis technologies.

Keywords: hydrogen evolution reaction; catalytic trends; acidic media; neutral media; alkaline media



Citation: Gebremariam, G.K.; Jovanović, A.Z.; Dobrota, A.S.; Skorodumova, N.V.; Pašti, I.A. Hydrogen Evolution Volcano(es)—From Acidic to Neutral and Alkaline Solutions. *Catalysts* **2022**, *12*, 1541. <https://doi.org/10.3390/catal12121541>

Academic Editor: Svetlana B. Štrbac

Received: 12 November 2022

Accepted: 28 November 2022

Published: 30 November 2022

Publisher's Note: MDPI stays neutral with regard to jurisdictional claims in published maps and institutional affiliations.



Copyright: © 2022 by the authors. Licensee MDPI, Basel, Switzerland. This article is an open access article distributed under the terms and conditions of the Creative Commons Attribution (CC BY) license (<https://creativecommons.org/licenses/by/4.0/>).

1. Introduction

Hydrogen evolution reaction (HER) has always had a special place in electrochemistry, but nowadays, it has gained even more attention due to the global energy crisis. As hydrogen is sought as the fuel of the future, finding economical ways for its production would solve the existing problems. This particularly relates to green hydrogen production via water electrolysis, where renewable energy sources are used to produce high-purity hydrogen. However, green hydrogen is still rather expensive. Thus, finding new, efficient catalysts for its production is necessary.

Understanding HER activity trends can help us in this search, and the best example is the HER volcano curve. In the original formulation, it was shown that HER exchange current densities were correlated with hydride formation energies of different metals [1]. Another formulation of HER volcano comes from the group of Nørskov et al. [2], where literature data for HER exchange current densities in acidic media were correlated to the theoretically calculated hydrogen binding energies. However, this approach was criticized [3], suggesting it was overly simplistic. Moreover, it was suggested that there was no volcano if oxide-covered metals were removed (W, Mo, Ta, Ti, and Nb from the “original” volcano) and that the reaction rate does not decrease for highly exothermic hydrogen adsorption [4]. Nevertheless, the HER volcano curve represents an appealing depiction of HER activity trends. Therefore, it is widely used in the community to search for new HER catalysts by pinpointing materials with optimal hydrogen binding energies, even

though such an approach might not be theoretically well-justified in each particular case. In fact, HER volcano for alkaline media, using calculated hydrogen binding energies, was demonstrated in 2013 [5] and received tremendous attention from the scientific community.

However, there is an important question of whether the volcano shape of the curve is preserved in different electrolytes and, particularly, what the trends are in pH-neutral solutions. Namely, for pH-neutral solutions, a systematic analysis is missing. This question is especially important for seawater electrolysis technologies, which suffer from many issues [6]. Moreover, while the effects of surface oxidation have been considered and discussed for the acidic solutions [4], a detailed analysis for the case of alkaline solutions is lacking. On the other hand, it is known that in an alkaline media, surface oxidation can boost H_2O dissociation at a metal | oxide interface, boosting HER in this way [7,8]. Thus, there is a question if such an interface engineering could help us to detach from the HER volcano or shift its apex from platinum to more affordable catalysts.

In the present work, we communicate our results on the HER activity trends in 7 different electrolytes ($0.1 \text{ mol dm}^{-3} \text{ HClO}_4$, $0.1 \text{ mol dm}^{-3} \text{ HCl}$, $0.5 \text{ mol dm}^{-3} \text{ NaCl}$, $1 \text{ mol dm}^{-3} \text{ KH}_2\text{PO}_4$, $0.1 \text{ mol dm}^{-3} \text{ KOH}$, $0.1 \text{ mol dm}^{-3} \text{ LiOH}$, and $1 \text{ mol dm}^{-3} \text{ KOH}$), in which we measured HER activity for nine metals (Ag, Au, Co, Cr, Fe, Ni, Pt, W, and Zn). We took special care to reduce oxide formation and measure HER activity on clean metallic surfaces (as much as possible). Moreover, for selected cases, we measured the HER activity after the surface oxidation and briefly discussed its effects, splitting them into trivial and nontrivial ones. Overall, we find that volcano curve shapes are present in all the electrolytes, while surface oxidation can significantly affect HER activity. Furthermore, the effects of surface oxidation depend on the particular metal-electrolyte combination. The data presented here are the starting point for the forthcoming work focusing on a detailed analysis of HER activity trends in a wide pH range and the effects of metal | oxide interface engineering.

2. Results

In order to establish trends in catalytic activities over the series of investigated polycrystalline metals, we determined HER overpotentials for the current density of $-100 \mu\text{A cm}^{-2}_{\text{real}}$. This value was not arbitrarily chosen, but it was selected based on the currently used and widely accepted measure of HER activity established by McCrory et al. [9], namely $-10 \text{ mA cm}^{-2}_{\text{geom}}$. In the mentioned work, high surface area catalysts are compared using this value, and their roughness factors (RFs) are of the order of 10^2 . This means the comparison can be made using roughly 10^2 times lower current densities if normalized to the electrochemically active surface area. We note that the trend is generally preserved for a wide range of current densities but that the exact position of a given metal on a volcano plot depends on the chosen current density. Calculated RFs of the electrodes used in this work are given in Appendix A. When constructing volcano curves, we used (i) the I-E curves obtained on the freshly polished electrodes (see Figures S1 and S2 for HER polarization curves in $0.1 \text{ mol dm}^{-3} \text{ KOH}$ and HCl) and (ii) the I-E curves obtained upon cycling an electrode to high anodic potentials (approx. $+1.4 \text{ V vs. RHE}$ in a given solution). Thus, the second case relates to HER activities over oxidized surfaces if the oxide layer is not easily reducible under HER conditions. We note that the oxidation steps are not performed in every solution and for all the electrodes, but just in cases that we considered particularly interesting to investigate. Figure 1 presents HER volcanoes in acidic solutions, while Figures 2 and 3 give HER volcanoes in neutral and alkaline solutions. Experimental data on HER overpotentials were correlated to the DFT-calculated hydrogen binding energies (HBE). The HBE data set was obtained by collecting available literature data (periodic DFT calculations) and averaging them, while for some metals where we could not find reliable literature data (Cr and Zn), we performed our own calculations. The data are summarized in Appendix A.

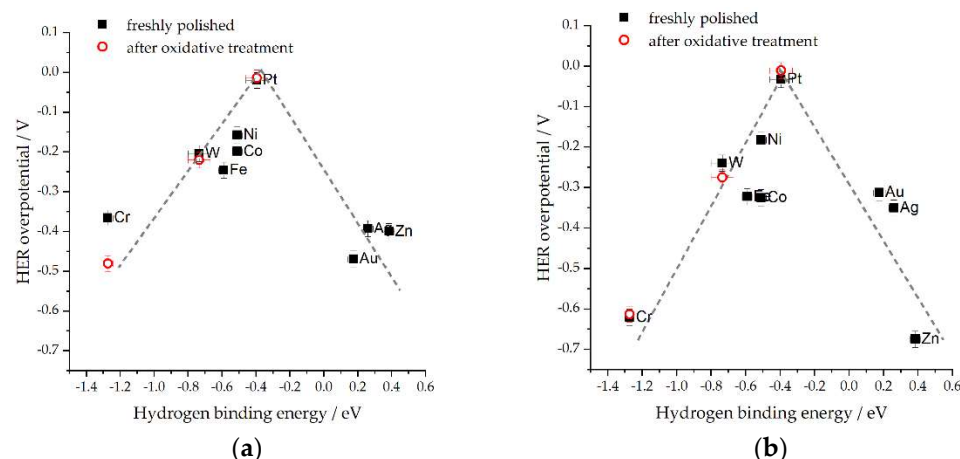


Figure 1. The HER volcanoes in acidic media: (a) $0.1 \text{ mol dm}^{-3} \text{ HClO}_4$; (b) $0.1 \text{ mol dm}^{-3} \text{ HCl}$. Squares represent freshly polished electrodes, while circles are for the electrodes after oxidative treatment.

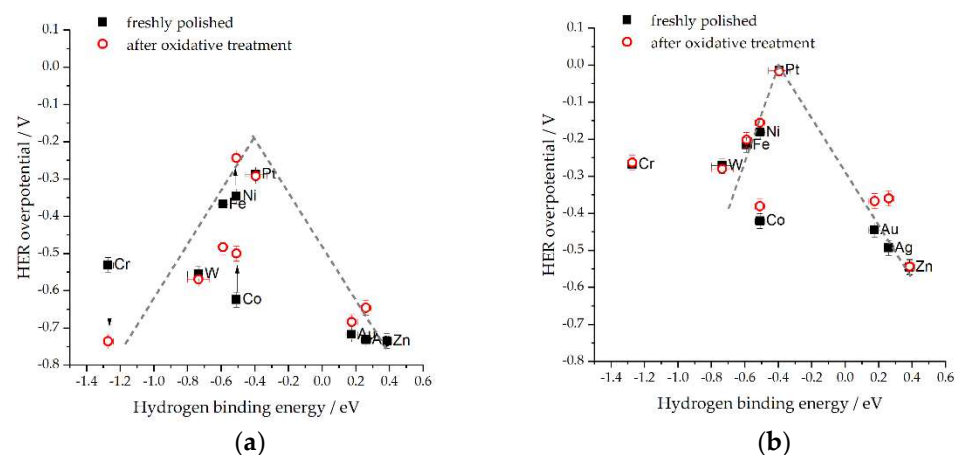


Figure 2. The HER volcanoes in neutral media: (a) $0.5 \text{ mol dm}^{-3} \text{ NaCl}$ (simulated sea water); (b) $1 \text{ mol dm}^{-3} \text{ KH}_2\text{PO}_4$ (in both cases, pH was adjusted to 7.0). Squares represent freshly polished electrodes, while circles are for the electrodes after oxidative treatment. In the case of the NaCl solution, arrows indicate the most prominent activity changes.

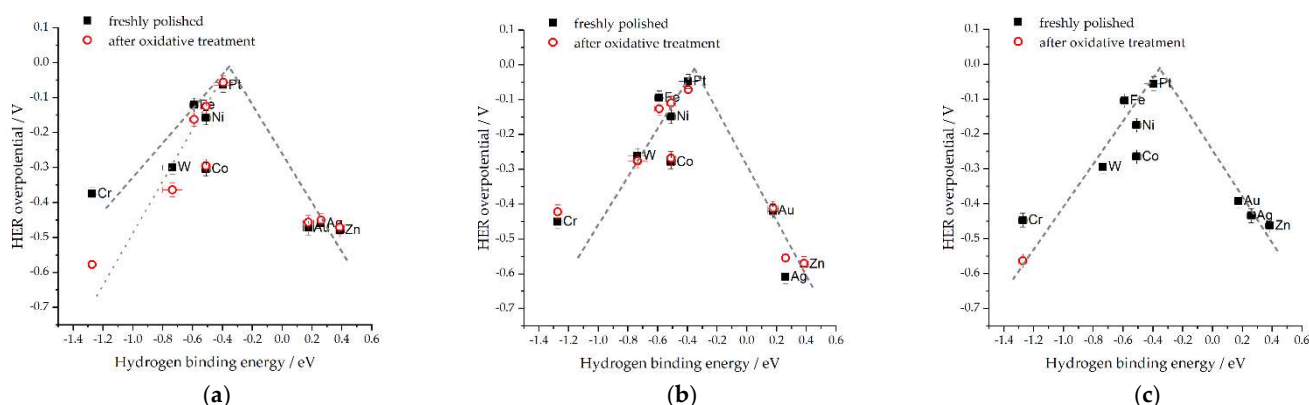


Figure 3. The HER volcanoes in alkaline media: (a) $0.1 \text{ mol dm}^{-3} \text{ KOH}$; (b) $0.1 \text{ mol dm}^{-3} \text{ LiOH}$; (c) $1 \text{ mol dm}^{-3} \text{ KOH}$. Squares represent freshly polished electrodes, while circles are for the electrodes after oxidative treatment. In the case of $0.1 \text{ mol dm}^{-3} \text{ KOH}$, one can draw two strongly binding branches of the HER volcano, depending on the presence of oxide on the surface.

Evidently, the volcano shape of the HER overpotential-HBE curve is mainly preserved in all seven solutions we investigated, particularly around the apex. However, it is also

quite clear that the electrolytes have a rather large impact on the “absolute” activities of investigated metals, while exposing the electrodes to the oxidizing conditions also has a tremendous impact on their activities. This issue is particularly important in the case of neutral solutions, where the strong binding branch of the volcano is deformed, and the hydrogen binding energy seems to have a less determining role compared to the acidic and alkaline solutions.

3. Discussion

Some general conclusions can be extracted from the overall trends in HER activities. First of all, in the case of freshly polished electrodes, where we took care to minimize the presence of oxides on the catalyst surfaces, platinum is the most active metal in all the cases. Moreover, as Pt oxides are easily reducible in all the solutions, the effects of its exposure to anodic potentials on the HER activity are minor. Moreover, in acidic solutions (Figure 1), HCl and HClO₄, Pt shows negligible HER overpotential, as expected, while in alkaline solutions, the overpotential is larger (around −0.1 V in agreement with previous studies [9,10]) as the slow water dissociation step hinders HER. The HER overpotential range spans over a wider window in HCl compared to HClO₄ as there is likely poisoning of the metal surfaces by chloride. This effect is especially prominent in pH-neutral solutions where the volcano apex is shifted by almost −0.3 V in NaCl (simulated sea water) compared to 1 mol dm^{−3} KH₂PO₄ solution (where Pt shows very small HER onset potential).

In alkaline media (Figure 3) volcano shape is well-defined. Therefore, without going deeper into the origin of such catalytic activity trends, it can be said that hydrogen binding energy can serve as a good descriptor for HER activity in alkaline media, such as in acidic ones. This conclusion is not surprising, as it has already been shown that HER volcano is preserved in alkaline solutions when using hydrogen binding energies as the descriptor [5]. However, some peculiarities in HER activities can also be outlined, particularly in neutral solutions. This case is certainly the most interesting as HER volcanoes’ strong binding branches seem flattened (the cases of W or Cr), while Co shows surprisingly low activities in both pH-neutral solutions investigated here. This result seems to align with the considerations given in Ref. [4] regarding the activity of metals where hydrogen adsorption is highly exothermic. Nevertheless, the situation gets more complicated when the activities after the oxidation treatment are considered.

To describe the effects of surface oxidation, we believe these could be split into trivial and nontrivial ones. The trivial effects of surface oxidation relate to the cases where the metal is actively dissolved during the potential cycling coupled with electrode rotation. For example, this is the case of Ag in the NaCl solution where AgCl is formed and reduced during the cycling, leading to the increase in the specific surface area, i.e., RF, and activity (please note that the roughness factors have been determined only immediately after the electrode polishing, and not during the measurements protocol). A similar trend can be considered for W, as W-oxides actively dissolve in alkaline solutions [11], leading to the electrochemical polishing of the electrode and the reduction of RF (and consequently the electrode activity), Figure 3. In contrast, the nontrivial cases of activity change are associated with the buildup of the stable oxide layer, where two possibilities arise. The first one is that the oxide layer is stable and blocks HER due to its inherent inactivity towards HER and/or insulating properties. This situation is likely operative in the case of Cr in most of the investigated solutions (and W in acidic solutions, although the effect is less visible for low current densities used here to benchmark HER activities). For this reason, the strong-binding branch is drawn with some uncertainty, and stable oxides on valve metals can likely disrupt the volcano shape if there is no special care to avoid or reduce oxide presence, which is, in some cases, impossible to do to the full extent. Such drastic effects of the HER inhibiting oxide layer are depicted in Figure 4 for the case of Cr in the HClO₄ and NaCl solution. Naturally, one can ask why there is no such extremely prominent effect in HCl at low current densities, but there is no simple answer to this question. The activity in the HCl solution is de facto much lower than in HClO₄, but the effects of the oxidation are

not as prominent, at least at low HER current densities (Figure 1b). At this point, we can only speculate that there are some differences in the states of the Cr oxide films formed in HClO_4 and NaCl solutions compared to the ones formed in the HCl solution. After all, it is obvious that the Cr oxide films formed in HClO_4 and NaCl are also not identical, based on the cyclic voltammograms of their formation (Figure 4, insets).

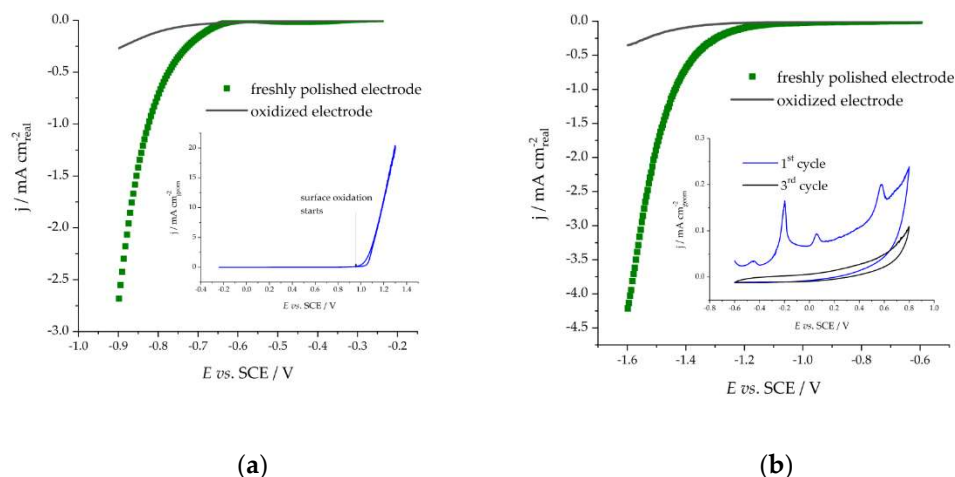


Figure 4. The HER polarization curve of the Cr electrode before and after oxidative treatment in (a) $0.1 \text{ mol dm}^{-3} \text{HClO}_4$ and (b) $0.5 \text{ mol dm}^{-3} \text{NaCl}$; insets show cycling voltammograms of the Cr electrode during which an irreversible oxide layer formation takes place. Roughly 10 times higher current at anodic vertex potential is observed in the HClO_4 solution compared to the NaCl solution.

The second possibility is that the oxide layer actually boosts HER activity. This scenario can be understood in terms of the enhanced rate of water dissociation at the metal | oxide interface [7,8]. Such an effect is operative for Ni and Co in the pH-neutral and alkaline solutions, while for Fe, the effect is either minor or negative. The HER boosting is especially prominent in the simulated seawater (Figure 5), where the activity of Ni becomes higher than that of Pt after the oxidative treatment. Thus, the volcano apex shifts towards Ni (Figures 2a and 5), which is not only the consequence of the increased activity of Ni but also the active poisoning of Pt with chloride and slow(er) H_2O dissociation on the oxide-free chloride-poisoned Pt surface compared to Ni | Ni-oxide interface.

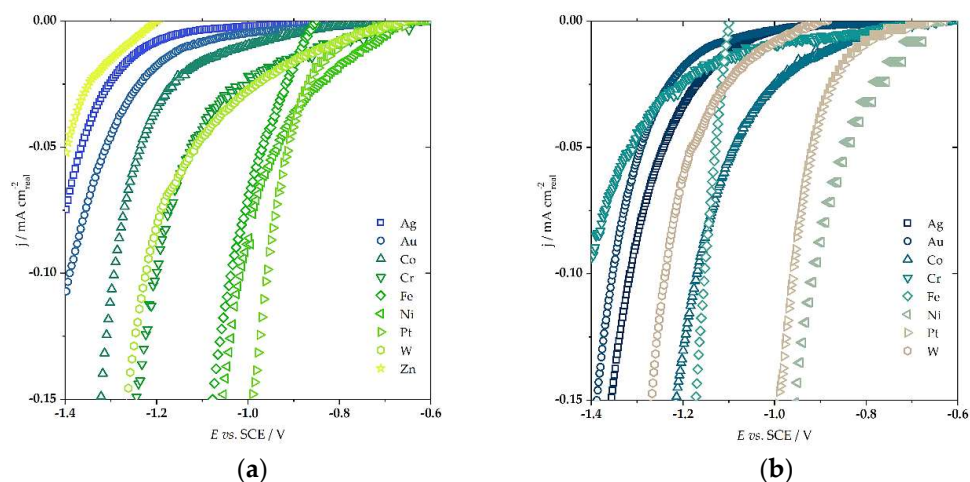


Figure 5. The HER polarization curves in $0.5 \text{ mol dm}^{-3} \text{NaCl}$ of (a) freshly polished electrodes and (b) after oxidation to high anodic potentials. Please note that the HER activity of Zn was not possible to determine due to very active dissolution during the anodic treatment. Observe the inversion of Pt and Ni activity after the oxidative treatment.

Overall, the presented results show that volcano-type relationships for HER hold in a wide pH range, with platinum being on the top of all volcano curves if freshly polished surfaces are considered, with as much as possible reduced oxide content under described experimental conditions. However, there are more or less subtle electrolyte effects determined by the presence of strongly adsorbing ions (chloride) and structure-making/breaking effects of cations which are not discussed here [12–15]. Our primary aim was to communicate an important finding that hydrogen binding energies present good descriptors for HER activities in practically the entire pH range. On the other hand, surface oxidation is an additional factor that must be considered. If special care is not taken, it can distort the volcano's shape, making it look better or worse, depending on the electrolyte. Furthermore, oxide formation and its effects on the HER activity are also electrolyte-dependent and need to be considered if one aims to boost HER via metal | oxide interface engineering.

Several additional effects are potentially rather important. First of all, the impurities could affect the measured HER activities. From the fundamental point of view, this would alter the position of a given metal at the volcano. As we performed the measurements in an identical way, the effect should be the same for all the metals studied in a given solution. From the practical point of view (for example, industrial applications), this could be significant if some metal impurities are present and deposited on the electrode during HER, changing the electrode's surface composition and thus affecting the activity. This issue is certainly worthy of further investigation, as it is unclear if the presence of impurities can negatively or positively affect the HER activity. However, we note that chloride was addressed here in both acidic and pH-neutral conditions, and the effects are particularly prominent in pH-neutral solutions. Thus, the effects of impurities should also be pH-dependent. This conclusion might be linked to the pH dependence of hydrogen binding energies [16], which are shown to decrease monotonously with the increasing pH of the electrolyte. The effect is seen as responsible for pH-dependent HER electrochemistry. However, considering the main findings of this work, this is not of primary importance. Namely, we show that novel catalysts can be screened using H binding energies, calculated at the metal | vacuum interface, irrespective of the pH of the electrolyte in which HER will take place. Thus, it is (only) important to find the catalyst which binds H_{ads} with similar strength as Pt. Depending on the pH of the solution, H binding energies will shift systematically, and the activity should remain close to that of Pt. The same applies to the presence of oxides. One can invest an effort to reduce their presence, but this might not be possible to a full extent. However, the adsorption energies of simple adsorbates scale to each other [2], and a catalyst that binds H_{ads} similarly to Pt should behave as Pt in terms of surface oxidation as well. Thus, searching for novel catalysts that bind H_{ads} as Pt also means identifying catalysts with similar oxophilicity as Pt.

4. Materials and Methods

4.1. Electrochemical Measurements

Electrochemical measurements were performed on polycrystalline metallic rotating disk electrodes (RDE) with a Teflon diameter of 10 mm. Disks of Ag, Au, Co, Fe, Pt, and W had diameters of 3 mm, the Ni disk had a diameter of 3.2 mm, while Cr and Zn disks had a diameter of 5 mm. RDE electrodes were in-house made, while metals were at least 99.95% (except Cr with 99.7%), purchased from Goodfellow Cambridge Ltd. (Cambridge, UK). Before the measurements, each disk was polished to a mirror finish with alumina powder and then sonicated for 15 s. Then, the disks were rinsed with the working solution and quickly transferred to the electrochemical cell. The measurements started immediately after the transfer to the cell to minimize oxide formation on the metal surfaces.

Electrochemical measurements were conducted using IVIUM Vetex. One in a one-compartment three-electrode glass electrochemical cell with a double-junction Saturated Calomel Electrode (SCE) as a reference electrode. While glass could leach silicates in alkaline solutions during the extended experiment, such effects can be disregarded here due to short experiments for each electrode (<10 min). A graphite rod (acidic solutions) or

a 3×3 cm Ni foam (pH neutral and alkaline solutions) was used as a counter electrode. As the electrolytic solution, $0.1 \text{ mol dm}^{-3} \text{ HClO}_4$, $0.1 \text{ mol dm}^{-3} \text{ HCl}$, $0.5 \text{ mol dm}^{-3} \text{ NaCl}$, $1 \text{ mol dm}^{-3} \text{ KH}_2\text{PO}_4$, $0.1 \text{ mol dm}^{-3} \text{ KOH}$ solution, $0.1 \text{ mol dm}^{-3} \text{ LiOH}$, and $1 \text{ mol dm}^{-3} \text{ KOH}$ were prepared with ultrapure deionized water (Sigma Aldrich, St. Louis, MO, USA, chemicals were used; hydroxides were anhydrous, with $\geq 99.9\%$ trace metal basis). All the measurements were conducted at room temperature. In this work, potentials are referred to as SCE, and to calculate HER overpotentials, potentials are converted to the Reversible Hydrogen Electrode (RHE) scale as $E_{\text{RHE}} = E_{\text{SCE}} + 0.244 \text{ V} + 0.059 \text{ V} \times \text{pH}$. Electrolyte resistance was corrected using hardware settings, up to 75 % of the resistance value, determined using single-point impedance measurement at 0 V vs. RHE (100 kHz). HER measurements were conducted using cyclic voltammetry at a potential sweep rate of 10 mV s^{-1} . Before the potential sweep, the electrode potential was maintained at -1 V , -0.6 V , and -0.24 V vs. SCE, for alkaline, pH-neutral, and acidic solutions, respectively, until the current density dropped below $1 \mu\text{A cm}^{-2}$. Then, three cycles were performed to deep negative potentials, after which the electrode was cycled between 0 and $+1.4 \text{ V}$ vs. RHE at 20 mV s^{-1} . Then, the HER measurement was repeated as described. The electrodes were constantly under the potential control and were not allowed to relax to the open circuit potential. During the measurements protocol, the electrodes were constantly rotated at 1800 rpm to remove any H_2 bubbles formed on the surface.

RF measurements were conducted on freshly polished electrodes using cyclic voltammetry in a narrow potential window, except for Fe and Pt. Measurements were conducted in $1 \text{ mol dm}^{-3} \text{ KOH}$ solution by cycling the electrodes between -0.1 and 0 V vs. RHE. Before the measurements, the electrodes were subjected to intensive HER at deep negative potentials to reduce oxide content. Electrode capacitance, determined from the slope of the current vs. potential scan rate line, was divided by $20 \mu\text{F cm}^{-2}$ [17,18] to obtain the real electrochemically active surface area (ESA). Then, the measured HER currents were normalized by ESA. RF was determined as the ratio of ESA and the geometrical cross-section of a disk. In the case of Fe, this method led to a large scattering of the current vs. potential scan rate resulting in unreliable determination of the RF. Thus, we determined the roughness factor for the Fe disk using impedance spectroscopy. The disk was exposed to HER at -0.3 V vs. RHE in $1 \text{ mol dm}^{-3} \text{ KOH}$, and the impedance spectrum was recorded in the frequency range of 0.1 Hz to 100 kHz . The capacitance of the electrode was determined by fitting the spectra, and ESA was obtained by dividing capacitance with $20 \mu\text{F cm}^{-2}$, assuming an oxide-free surface. Finally, for Pt, RF and ESA were determined using cyclic voltammetry in $0.1 \text{ mol dm}^{-3} \text{ HClO}_4$. ESA was determined by integrating the hydrogen underpotential deposition/H desorption peaks and subsequent dividing of the charge under peaks by $210 \mu\text{C cm}^{-2}$ [18]. We note that there are many proposed methods for ESA determination, such as the one based on adsorption capacitance, which seems particularly suitable for some metals studied here [19]. However, this method is not confirmed for the entire series of catalysts studied here. Thus, we based ESA determination on capacitance measurements where possible or where the standard procedure does not exist, like for Pt.

4.2. DFT Calculations

The first-principle DFT calculations were performed using the Vienna ab initio simulation code (VASP) [20–22]. The Generalized Gradient Approximation (GGA) in the parametrization by Perdew, Burk, and Ernzerhof [23] combined with the projector augmented wave (PAW) method was used [24]. Cut-off energy of 350 eV and Gaussian smearing with a width of $\sigma = 0.025 \text{ eV}$ for the occupation of the electronic levels were used. The (2×2) Zn (0001) and Cr (110) surfaces were investigated. Four-layer slabs were used. Atomic hydrogen adsorption was investigated at 0.25 monolayer coverage, and the hydrogen binding energy (HBE) was calculated vs. isolated H_2 molecule as:

$$\text{HBE} = E_{\text{Surf} + \text{H}} - E_{\text{Surf}} - 1/2E_{\text{H}_2}, \quad (1)$$

where $E_{\text{Surf} + \text{H}}$, E_{Surf} , and E_{H_2} stand for the total energy of the surface with an adsorbed hydrogen atom, the total energy of the clean surface, and the total energy of an isolated H_2 molecule, respectively. For other metals, we took literature data calculated at the same level of theory using periodic DFT calculations. The data are assembled in Appendix A, Table A1.

5. Conclusions

The present work is aimed to communicate the systematic analysis of the HER catalytic trends over the polycrystalline metallic surfaces in different solutions with pH ranging from highly acidic to highly alkaline. When HER overpotentials (determined at the current density of $-100 \mu\text{A cm}^{-2}_{\text{real}}$) are correlated to the calculated hydrogen binding energies, HER volcano curves are observed in all the solutions. For any given metal, one can consider that electrolyte effects are present, but in all the cases when freshly polished surfaces are considered, Pt remains the most active catalyst. On the other hand, surface oxidation can significantly affect the HER activities. Considering the nontrivial effects of surface oxidation, the effects are seen in HER blockage (Cr and W) or HER activity boosting. The latter case is particularly related to Ni and Co in alkaline and especially pH-neutral solutions, which can be ascribed to the enhanced water dissociation at the metal|oxide interface. In the case of Ni, the effect is so pronounced in NaCl solution that, after oxidation, it makes it more active than Pt. However, the volcano shape is largely preserved. We believe that hydrogen binding energy can be used to identify highly active HER catalysts independent of the pH, seemingly without searching for deep theoretical justification of the observed trends (which is more than needed). Nevertheless, to completely understand the catalytic trends and the electrolyte effects, one must consider water dissociation in pH-neutral and alkaline solutions and the presence of strongly adsorbing ions.

Our future work will be directed to analyzing the mentioned effects and a detailed kinetic analysis of the presented data. Additionally, it is necessary to address the deformation of the strong binding branch of the HER volcanoes and put it in a proper theoretical context. The oxidation effects are particularly important as they can change our perception of the HER activity trends, possibly allowing us to detach from the HER volcano and find more efficient and economically attractive catalysts.

Supplementary Materials: The following supporting information can be downloaded at: <https://www.mdpi.com/article/10.3390/catal12121541/s1>, Figure S1: HER polarization curves in 0.1 mol dm^{-3} KOH solution (freshly polished electrodes); Figure S2: HER polarization curves in 0.1 mol dm^{-3} HCl solution (freshly polished electrodes).

Author Contributions: Conceptualization, I.A.P.; methodology, G.K.G., A.Z.J. and I.A.P.; validation, N.V.S. and I.A.P.; formal analysis, G.K.G., A.Z.J. and A.S.D.; investigation, G.K.G., A.Z.J. and A.S.D.; resources, N.V.S. and I.A.P.; data curation, A.S.D. and I.A.P.; writing—original draft preparation, A.S.D. and I.A.P.; writing—review and editing, N.V.S. and I.A.P.; funding acquisition, N.V.S. and I.A.P. All authors have read and agreed to the published version of the manuscript.

Funding: This research was funded by the Science Fund of the Republic of Serbia (PROMIS project RatioCAT) and the Ministry of Education, Science, and Technological Development of the Republic of Serbia (Contract No. 451-03-68/2020-14/200146). I.A.P. is indebted to the Research Fund of the Serbian Academy of Sciences and Arts, project F-190, for supporting this study. The computations and data handling were enabled by resources provided by the Swedish National Infrastructure for Computing (SNIC) at the National Supercomputer Centre (NSC) at Linköping University, partially funded by the Swedish Research Council through grant agreement No. 2018-05973.

Data Availability Statement: Data are available upon reasonable request.

Acknowledgments: I.A.P. would like to thank Slavko V. Mentus, University of Belgrade—Faculty of Physical Chemistry, for helpful discussions.

Conflicts of Interest: The authors declare no conflict of interest.

Appendix A

Table A1. Roughness factors and hydrogen binding energies (HBE) for the investigated metals. Hydrogen binding energies were obtained by averaging data found in Refs. [2,5,25,26].

Title 1	Title 2	HBE/eV ¹
Ag	17.7 ± 0.9	0.26 ± 0.03
Au	9 ± 2	0.175 ± 0.035
Co	9.9 ± 1.5	−0.51 ± 0.03
Cr	2.4 ± 0.2	−1.273 ± 0.03
Fe	3.4 ± 0.2	−0.59 ± 0.03
Ni	2.7 ± 0.2	−0.51 ± 0.03
Pt	6 ± 1	−0.395 ± 0.065
W	2.1 ± 0.2	−0.735 ± 0.065
Zn	24 ± 4	0.39 ± 0.03

¹ For Cr and Zn, we assumed the uncertainty of the calculated HBE to be 30 meV, which is a typical accuracy of the used computational approach and also matches the data scattering for other metals.

References

- Trasatti, S. Work Function, Electronegativity, and Electrochemical Behaviour of Metals: III. Electrolytic Hydrogen Evolution in Acid Solutions. *J. Electroanal. Chem. Interfacial Electrochem.* **1972**, *39*, 163–184. [\[CrossRef\]](#)
- Nørskov, J.K.; Bligaard, T.; Logadottir, A.; Kitchin, J.R.; Chen, J.G.; Pandelov, S.; Stimming, U. Trends in the Exchange Current for Hydrogen Evolution. *J. Electrochem. Soc.* **2005**, *152*, J23–J26. [\[CrossRef\]](#)
- Schmickler, W.; Trasatti, S. Comment on “Trends in the Exchange Current for Hydrogen Evolution” [*J. Electrochem. Soc.*, *152*, J23 (2005)]. *J. Electrochem. Soc.* **2006**, *153*, L31–L32. [\[CrossRef\]](#)
- Quaino, P.; Juarez, F.; Santos, E.; Schmickler, W. Volcano plots in hydrogen electrocatalysis—Uses and abuses. *Beilstein J. Nanotechnol.* **2014**, *5*, 846–854. [\[CrossRef\]](#)
- Sheng, W.; Myint, M.; Chen, J.G.; Yan, Y. Correlating the hydrogen evolution reaction activity in alkaline electrolytes with the hydrogen binding energy on monometallic surfaces. *Energy Environ. Sci.* **2013**, *6*, 1509–1512. [\[CrossRef\]](#)
- Khan, M.A.; Al-Attas, T.; Roy, S.; Rahman, M.M.; Ghaffour, N.; Thangadurai, V.; Larter, S.; Hu, J.; Ajayan, P.M.; Kibria, G. Seawater electrolysis for hydrogen production: A solution looking for a problem? *Energy Environ. Sci.* **2021**, *14*, 4831–4839. [\[CrossRef\]](#)
- Subbaraman, R.; Tripkovic, D.; Chang, K.-C.; Strmcnik, D.; Paulikas, A.P.; Hirunsit, P.; Chan, M.; Greeley, J.; Stamenkovic, V.; Markovic, N.M. Trends in Activity for the Water Electrolyser Reactions on 3d M(Ni,Co,Fe,Mn) Hydr(Oxy)Oxide Catalysts. *Nat. Mater.* **2012**, *11*, 550–557. [\[CrossRef\]](#)
- Danilovic, N.; Subbaraman, R.; Strmcnik, D.; Chang, K.-C.; Paulikas, A.P.; Stamenkovic, V.R.; Markovic, N.M. Enhancing the Alkaline Hydrogen Evolution Reaction Activity through the Bifunctionality of Ni(OH)₂/Metal Catalysts. *Angew. Chem. Int. Ed.* **2012**, *51*, 12495–12498. [\[CrossRef\]](#)
- McCrory, C.C.L.; Jung, S.; Ferrer, I.M.; Chatman, S.M.; Peters, J.C.; Jaramillo, T.F. Benchmarking Hydrogen Evolving Reaction and Oxygen Evolving Reaction Electrocatalysts for Solar Water Splitting Devices. *J. Am. Chem. Soc.* **2015**, *137*, 4347–4357. [\[CrossRef\]](#)
- Jovanović, A.Z.; Bijelić, L.; Dobrota, A.S.; Skorodumova, N.V.; Mentus, S.V.; Pašti, I.A. Enhancement of Hydrogen Evolution Reaction Kinetics in Alkaline Media by Fast Galvanic Displacement of Nickel with Rhodium—From Smooth Surfaces to Electrodeposited Nickel Foams. *Electrochim. Acta* **2022**, *414*, 140214. [\[CrossRef\]](#)
- Pašti, I.A.; Lazarević-Pašti, T.; Mentus, S. Switching between Voltammetry and Potentiometry in Order to Determine H⁺ or OH[−]—Ion Concentration over the Entire PH Scale by Means of Tungsten Disk Electrode. *J. Electroanal. Chem.* **2012**, *665*, 83–89. [\[CrossRef\]](#)
- Ding, X.; Garlyyev, B.; Watzele, S.A.; Kobina Sarpey, T.; Bandarenka, A.S.; Ding, X.; Garlyyev, B.; Watzele, S.A.; Kobina Sarpey, T.; Bandarenka, A.S. Spotlight on the Effect of Electrolyte Composition on the Potential of Maximum Entropy: Supporting Electrolytes Are Not Always Inert. *Chem. A Eur. J.* **2021**, *27*, 10016–10020. [\[CrossRef\]](#) [\[PubMed\]](#)
- Taji, Y.; Zagalskaya, A.; Evazzade, I.; Watzele, S.; Song, K.-T.; Xue, S.; Schott, C.; Garlyyev, B.; Alexandrov, V.; Gubanova, E.; et al. Alkali Metal Cations Change the Hydrogen Evolution Reaction Mechanisms at Pt Electrodes in Alkaline Media. *Nano Mater. Sci.* **2022**, *in press*. [\[CrossRef\]](#)
- Subbaraman, R.; Tripkovic, D.; Strmcnik, D.; Chang, K.C.; Uchimura, M.; Paulikas, A.P.; Stamenkovic, V.; Markovic, N.M. Enhancing Hydrogen Evolution Activity in Water Splitting by Tailoring Li⁺-Ni(OH)₂-Pt Interfaces. *Science (1979)* **2011**, *334*, 1256–1260. [\[CrossRef\]](#)
- Ledezma-Yanez, I.; Wallace, W.D.Z.; Sebastián-Pascual, P.; Climent, V.; Feliu, J.M.; Koper, M.T.M. Interfacial Water Reorganization as a PH-Dependent Descriptor of the Hydrogen Evolution Rate on Platinum Electrodes. *Nat. Energy* **2017**, *2*, 1–7. [\[CrossRef\]](#)

16. Zhu, S.; Qin, X.; Yao, Y.; Shao, M. PH-Dependent Hydrogen and Water Binding Energies on Platinum Surfaces as Directly Probed through Surface-Enhanced Infrared Absorption Spectroscopy. *J. Am. Chem. Soc.* **2020**, *142*, 8748–8754. [[CrossRef](#)]
17. Łukaszewski, M.; Soszko, M.; Czerwiński, A. Electrochemical Methods of Real Surface Area Determination of Noble Metal Electrodes-an Overview. *Int. J. Electrochem. Sci.* **2016**, *11*, 4442–4469. [[CrossRef](#)]
18. Trasatti, S.; Petrii, O.A. Real Surface Area Measurements in Electrochemistry. *Pure Appl. Chem.* **1991**, *63*, 711–734. [[CrossRef](#)]
19. Watzele, S.; Hauenstein, P.; Liang, Y.; Xue, S.; Fichtner, J.; Garlyyev, B.; Scieszka, D.; Claudel, F.; Maillard, F.; Bandarenka, A.S. Determination of Electroactive Surface Area of Ni-, Co-, Fe-, and Ir-Based Oxide Electrocatalysts. *ACS Catal.* **2019**, *9*, 9222–9230. [[CrossRef](#)]
20. Kresse, G.; Hafner, J. Ab Initio Molecular Dynamics for Liquid Metals. *Phys. Rev. B* **1993**, *47*, 558–561. [[CrossRef](#)]
21. Kresse, G.; Furthmüller, J. Efficiency of Ab-Initio Total Energy Calculations for Metals and Semiconductors Using a Plane-Wave Basis Set. *Comput. Mater. Sci.* **1996**, *6*, 15–50. [[CrossRef](#)]
22. Kresse, G.; Furthmüller, J. Efficient Iterative Schemes for Ab Initio Total-Energy Calculations Using a Plane-Wave Basis Set. *Phys. Rev. B* **1996**, *54*, 11169–11186. [[CrossRef](#)]
23. Perdew, J.P.; Burke, K.; Ernzerhof, M. Generalized Gradient Approximation Made Simple. *Phys. Rev. Lett.* **1996**, *77*, 3865–3868. [[CrossRef](#)] [[PubMed](#)]
24. Blöchl, P.E. Projector Augmented-Wave Method. *Phys. Rev. B* **1994**, *50*, 17953–17979. [[CrossRef](#)] [[PubMed](#)]
25. Ferrin, P.; Kandoi, S.; Nilekar, A.U.; Mavrikakis, M. Hydrogen Adsorption, Absorption and Diffusion on and in Transition Metal Surfaces: A DFT Study. *Surf. Sci.* **2012**, *606*, 679–689. [[CrossRef](#)]
26. Greeley, J.; Mavrikakis, M. Surface and Subsurface Hydrogen: Adsorption Properties on Transition Metals and Near-Surface Alloys. *J. Phys. Chem. B* **2005**, *109*, 3460–3471. [[CrossRef](#)]